



1

2 **Bakaano-Hydro (v1.1). A distributed hydrology-guided deep**
3 **learning model for streamflow prediction**

4

5 Confidence Duku^{1,2}

6 ¹Climate Resilience Team, Wageningen Environmental Research, Wageningen University & Research,
7 Wageningen, The Netherlands

8 ²Earth Systems and Global Change, Wageningen University & Research, P.O. Box 47, 6700AA,
9 Wageningen, The Netherlands

10

11



12 Abstract

13 Reliable streamflow prediction is fundamental to hydrological forecasting, water resources planning, and
14 climate adaptation. However, existing data-driven approaches often lack physical interpretability and
15 struggle to incorporate spatial heterogeneity and hydrological connectivity. Conversely, traditional process-
16 based models are limited by high calibration demands and structural uncertainty, especially in data-scarce
17 regions. These challenges underscore the need for hybrid frameworks that combine the strengths of
18 physically based modeling with the predictive capacity of machine learning. Here, I present Bakaano-Hydro,
19 a distributed hydrology-guided deep learning model for streamflow prediction. The model integrates a
20 gridded runoff generation method, a topographic flow routing scheme, and a temporal convolutional
21 network to capture both spatial and temporal hydrological dynamics. This architecture enables
22 incorporation of spatial heterogeneity and explicitly represents hydrological connectivity, while using
23 neural networks to learn streamflow dynamics and enhance predictive performance. Bakaano-Hydro's
24 performance is evaluated across six river basins spanning four continents, encompassing diverse climate
25 zones, land-use patterns, and hydrological regimes. Results indicate that Bakaano-Hydro demonstrates
26 robust performance in humid and snow-fed basins where saturation-excess runoff dominates, while
27 revealing key limitations in arid and semi-arid regions characterized by infiltration-excess processes.
28 Bakaano-Hydro advances the state of the art in data-driven hydrological modeling by integrating physical
29 realism with deep learning. Its modular and fully automated pipeline enables rapid deployment in data-
30 scarce regions, while maintaining high reliability and interpretability. These features make Bakaano-Hydro
31 a promising tool for operational forecasting, climate risk assessment, and adaptation planning across
32 diverse hydrological and socio-environmental contexts. The model code is publicly available at
33 <https://github.com/confidence-duku/bakaano-hydro> to facilitate reproducibility and community-driven
34 development.

35 1. Introduction

36 Streamflow prediction is pivotal for meeting societal needs and underpins various critical areas including
37 water resources management, hydropower, flood management, infrastructure planning and climate
38 adaptation (Palmer and Ruhi, 2019; Depetris, 2021; Herrera et al., 2017; Cassagnole et al., 2021; Golden et
39 al., 2025). Traditionally, physically based hydrological models have been the primary tool for simulating
40 streamflow, relying on process-based equations to describe hydrological processes (e.g. Arnold et al., 1998;
41 Hamman et al., 2018; Schaphoff et al., 2018; De Roo et al., 2000). However, these models require extensive
42 calibration, struggle with parameter uncertainty in data-scarce regions, and often exhibit biases due to



43 structural limitations (Herrera et al., 2022; Moges et al., 2021). Recently, deep learning models have
44 emerged as powerful alternatives, offering data-driven solutions that can learn complex streamflow-
45 generation relationships directly from observational data. In particular, Long Short-Term Memory (LSTM)
46 networks have demonstrated superior predictive performance compared to many conceptual and
47 physically based models (Hunt et al., 2022; Kratzert et al., 2019; Kratzert et al., 2018; Gauch et al., 2021;
48 Nearing et al., 2024; Arsenault et al., 2023). These LSTM-based models employ lumped modelling
49 approaches where an entire watershed is treated as a single computational unit. Meteorological forcings,
50 soil, topographic and land use data are aggregated or area-weighted over a catchment, and the model
51 outputs streamflow at the outlet. Architectural constraints of available sequence-based neural network
52 algorithms including LSTMs drive the adoption of lumped modelling approach. While these LSTMs are
53 effective for capturing temporal dependencies in hydrological time series, they are not inherently designed
54 to process gridded or spatially distributed data. As a result, these LSTM-based lumped modelling
55 approaches, which are the state-of-the art in data-driven hydrological modelling face critical limitations,
56 despite their demonstrated predictive performance. A primary concern is their inability to capture spatial
57 heterogeneity, particularly in large or complex basins where sub-basin variability in precipitation, land
58 cover, soil moisture, and terrain strongly influences runoff generation. Consequently, the predictive skill of
59 lumped data-driven models typically declines with increasing basin size (Hunt et al., 2022). Studies have
60 shown that incorporating spatial variability, particularly in rainfall inputs, can enhance the predictive
61 performance of lumped data-driven approaches (Wang and Karimi, 2022). Another major limitation is the
62 inability to represent upstream-downstream hydrological connectivity, a key driver of streamflow, flood
63 dynamics, water availability, and ecosystem stability. Without explicit representation of hydrological
64 connectivity, these models struggle to simulate localized hydrological responses, flow propagation, and the
65 impacts of land-use change on water resources, making them less applicable for flood forecasting, water
66 resource management, and ecosystem conservation.

67 In recent years, two types of approaches have emerged to integrate spatial heterogeneity into data-driven
68 streamflow prediction frameworks: hybrid process-based and data-driven models, and the use of
69 convolutional neural network. For example, Yu et al. (2024) employed a spatially recursive hybrid approach
70 that first trains lumped regional LSTM model to predict local streamflow at a subbasin outlet and
71 subsequently uses the predicted streamflow as input to a physics-based hydrological routing model to
72 predict streamflow at the larger basin outlet. This approach, while incorporating elements of spatial
73 variability, cannot explicitly model spatially varying hydrological processes such as runoff generation across
74 the basin. Anderson and Radić (2022), on the other hand, employed a purely data-driven approach

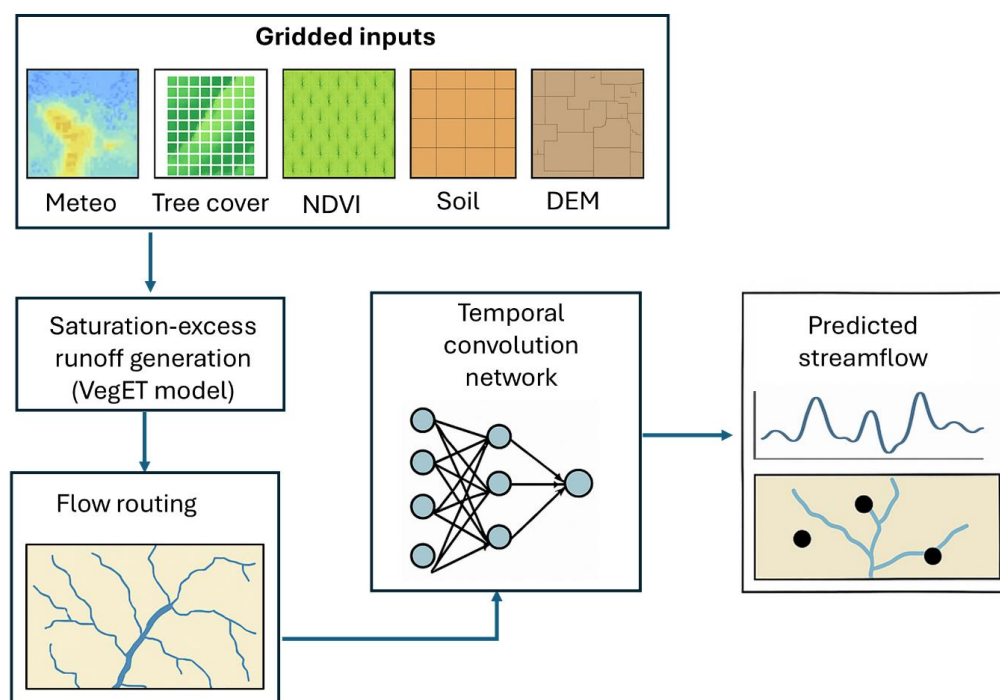


75 involving the use of convolutional long-short term memory (ConvLSTM) architectures to predict
76 streamflow. ConvLSTMs are essentially spatiotemporal neural networks that improve upon standard LSTMs
77 by incorporating spatial dependencies through convolutional operations (Shi et al., 2015). While this
78 architecture is well-suited for spatiotemporal sequence modeling, its application in hydrological contexts
79 remains limited. In particular, ConvLSTMs do not inherently respect the directional and hierarchical nature
80 of river networks governed by topography, and thus cannot enforce hydrologically consistent flow
81 accumulation and routing.

82 Consequently, despite progress in developing methods to better capture spatial heterogeneity in data-
83 driven hydrological modeling, existing approaches remain inadequate for fully distributed applications that
84 require representation of upstream–downstream connectivity and physically consistent flow propagation.
85 To address these limitations, I introduce Bakaano-Hydro, a distributed hydrology-guided deep learning
86 model for streamflow simulation. The term 'Bakaano' originates from a native Ghanaian language and
87 refers to river-side communities, who are seasonally at risk of fluvial flooding, a primary motivation for the
88 development of this tool. Bakaano-Hydro employs a serial hybridization approach and integrates a gridded
89 process-based rainfall-runoff method that captures spatial heterogeneity and dynamic interactions of
90 meteorological forcings and physiographic attributes generating spatially distributed runoff estimates; a
91 flow routing method propagating runoff through the river network based on topographic constraints to
92 preserve hydrological connectivity; and a sequential neural network that uses routed flow sequences
93 extracted at any point along a river network to predict streamflow. This approach ensures that primary
94 hydrological responses to climate, soil, topography, and vegetation interactions and changes are captured
95 by process-based components, enhancing interpretability while leveraging deep learning for pattern
96 recognition. I demonstrate the applicability, robustness and generalizability of Bakaano-Hydro in six case-
97 study basins of varying sizes, spanning four continents, hydroclimatic gradients and land-use patterns.

98 **2. Bakaano-Hydro model structure**

99 Bakaano-Hydro integrates a gridded runoff generation method, a topographic flow routing scheme, and a
100 temporal convolutional network to capture both spatial heterogeneity, hydrological connectivity and
101 temporal dynamics (Fig. 1). Bakaano-Hydro is scalable and operates at a daily time-step and at the spatial
102 resolution of the elevation data.



103

104 **Figure 1.** Conceptual diagram of the Bakaano-Hydro model. Meteo is meteorological variables; NDVI is
105 Normalised Difference Vegetation Index and DEM is Digital Elevation Model.

106

107 2.1. Runoff generation with a process-based method

108 The runoff generation phase in Bakaano-Hydro is designed to simulate spatiotemporal total runoff as a
109 function of climate, topography, vegetation, and soil interactions. Notably, runoff serves as an intermediate
110 variable in the model, with the primary focus on accurately representing its spatiotemporal variability
111 rather than capturing absolute runoff values. Runoff generation is based on the Vegetation ET (VegET)
112 method (Senay, 2008; Senay et al., 2023). VegET operates on gridded data and follows a one-dimensional
113 soil water balance framework, where each grid cell is modeled independently without explicit lateral water
114 flow. This gridded structure allows for seamless integration with meteorological datasets and remote
115 sensing products. Precipitation is partitioned into canopy interception, evapotranspiration, soil moisture
116 storage, and total runoff. A detailed description of VegET can be found in (Senay et al., 2023).

117 Interception is explicitly parameterized based on tree, herbaceous, and bare cover fractions. The
118 interception storage capacity varies dynamically with vegetation cover, ensuring that dense forested areas



119 intercept more rainfall than sparsely vegetated or bare soil regions. Actual evapotranspiration is estimated
120 as a function of the Normalized Difference Vegetation Index (NDVI) and reference evapotranspiration (PET).
121 NDVI, acts as a proxy for vegetation density and health, allowing the model to dynamically adjust
122 transpiration rates based on vegetation cover. In areas with abundant vegetation and sufficient soil
123 moisture, actual evapotranspiration approaches potential evapotranspiration, while in water-limited
124 regions, actual evapotranspiration is constrained by soil water availability. In Bakaano-Hydro, the
125 Hargreaves equation is used to estimate potential evapotranspiration (Hargreaves and Samani, 1985). In
126 VegET, soil water content is estimated as a function of soil properties such as wilting point, field capacity,
127 and saturation. Finally, runoff generation is estimated based on saturation-excess mechanism, where
128 precipitation that exceeds the soil's storage capacity contributes to runoff.

129 2.2. Topographic runoff routing through river network

130 The flow routing phase is pivotal to Bakaano-Hydro, bridging process-based runoff generation with data-
131 driven streamflow prediction. Daily total runoff generated by VegET method is routed to the river channel
132 network using the weighted flow accumulation method based on the multiple flow direction (MFD)
133 approach (Quinn et al., 1991). The MFD routing scheme distributes flow from each cell to up to eight
134 neighboring cells, with partitioning proportional to the elevation gradient between cells. For each study
135 domain or delineated basin, the resulting routed runoff is used to construct time-series inputs
136 corresponding to the spatial locations of hydrological observation stations. To account for potential
137 misalignments between observed station coordinates and the digital river network, a **coordinate snapping**
138 procedure is implemented. This step ensures that station coordinates are matched to the nearest river
139 segment, thereby minimizing spatial discrepancies and enhancing the reliability of extracted runoff signals.

140 It is important to note that this initial routing implementation does not explicitly account for hydrological
141 processes such as transmission losses, overbank flow, or in-channel travel time delays, which can influence
142 both the magnitude and timing of streamflow, particularly in arid and semi-arid regions or large river
143 systems. These processes are intentionally omitted at this stage, as the primary objective is to simulate
144 maximum potential daily flow at each hydrological point. These routed runoff time-series serve as inputs
145 to the subsequent deep learning stage, where temporal dependencies and additional hydrological
146 dynamics are learned directly from data.

147



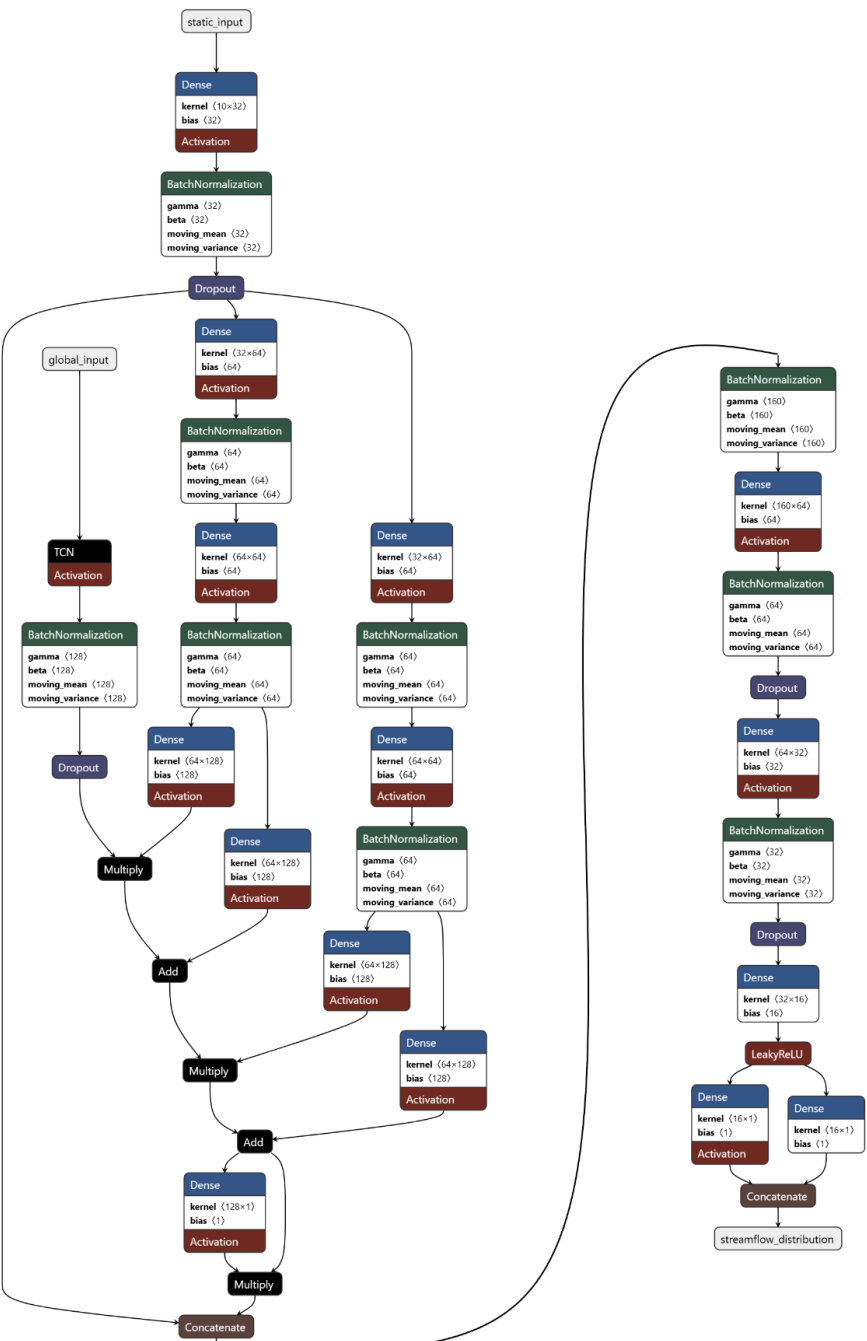
148 **2.3 Streamflow simulation with neural network**

149 Bakaano-Hydro employs Temporal Convolutional Networks (TCN) (Bai et al., 2018), attention mechanisms
150 (Luong et al., 2015), and Feature-wise Linear Modulation (FiLM) conditioning (Perez et al., 2018), to capture
151 the complex hydro-climatic dynamics governing streamflow (Fig.2). Importantly, Bakaano-Hydro is
152 designed as a single multitask model that can be trained on observations across a wide range of spatial
153 domains—from individual river basins to continental or even global extents. This enables the model to
154 learn shared representations across regions, improving its capacity for regional generalization and zero-
155 shot inference in ungauged or poorly monitored catchments. Such a design supports scalable streamflow
156 prediction and offers a unified approach for simulating hydrological dynamics across data-rich and data-
157 scarce regions alike.

158 **2.3.1 Input representation, preprocessing and feature engineering**

159 Bakaano-Hydro provides two architectural options for the neural network component. First, a two-input
160 branch neural network design that receives dynamic and static input data. In this design, the dynamic input
161 branch receives three features and the static branch, ten features. The dynamic input branch receives
162 routed runoff sequences extracted from a specified hydrological station or point along a river network; the
163 routed runoff sequences scaled by the upstream contributing area (i.e. number of upstream grid cells); and
164 also scaled by the depth-to-water index, a topographic metric reflecting subsurface hydrological storage.
165 The last two features facilitate generalization across catchments of varying scales and response times. To
166 ensure numerical stability during training, a quantile transformation is applied to the dynamic input
167 features, mapping them into percentile space using the empirical cumulative distribution function. This
168 transformation reduces sensitivity to extreme values and ensures the model learns from the full range of
169 hydrometeorological variability. The resulting normalized dynamic predictors are structured as a time
170 series over a fixed lookback period (i.e. 365 days), where streamflow for day t depends on this lookback
171 period allowing the model to learn temporal dependencies relevant to streamflow generation. The quantile
172 transformation is implemented globally within a basin i.e. on concatenated data from all stations together.

173 The static input branch comprises physiographic attributes representing watershed-scale controls on
174 runoff and routing. These variables, including slope, soil water holding capacity, soil saturation point,
175 fractional tree and herbaceous cover, are computed using a weighted flow accumulation approach and
176 normalized by the number of contributing grid cells at a hydrological station or specified point along a river
177 network. Additionally, sine and cosine transformations of latitude and longitude serve as spatial encodings.



178

179 **Figure 2.** Architecture of Bakaano-Hydro neural network component illustrating the two input-branch
180 design.



181 Features in the static input branch are scaled using the min-max scaling method. This normalization
182 method transforms each features into a range of [0,1], preserving the relative relationships between
183 different catchment attributes while ensuring that all features contribute proportionally to the learning
184 process.

185 The second option for the neural network component is the three-input branch design, which includes a
186 second dynamic input branch in addition to the aforementioned two. This second dynamic input branch
187 comprises only 1 feature, the routed runoff sequences scaled by the upstream contributing area. Unlike
188 the first dynamic input branch, quantile transformation is applied independently for each hydrological
189 station.

190 **2.3.2 Capturing temporal dependencies**

191 Unlike traditional recurrent architectures such as LSTMs, which process sequences sequentially, TCNs
192 leverage dilated causal convolutions, which allows for efficient parallel computation and stable gradient
193 propagation. TCNs also capture multi-scale temporal dependencies, e.g. short-term precipitation-driven
194 runoff and longer-term hydrological memory effects, preserving seasonal and interannual variability in
195 streamflow (Bai et al., 2018). In Bakaano-Hydro, a single TCN layer with dilation rates of 2,4,8,16,32,64,128
196 and 256 are employed. Batch normalization is used after TCN layer and mitigates the impact of skewed
197 streamflow distributions, while a dropout rate of 0.4 promotes generalization by reducing overfitting to
198 the training data (Ioffe and Szegedy, 2015; Srivastava et al., 2014).

199 In addition, attention mechanisms (Luong et al., 2015) are integrated in the architecture to dynamically
200 assign importance to the TCN outputs, ensuring that the most hydrologically relevant information is
201 emphasized in the prediction process. Standard convolutional and recurrent architectures process all time
202 steps with equal weight, which can dilute critical signals. The attention mechanism addresses this issue by
203 adaptively prioritizing key temporal features based on their contribution to streamflow response. Attention
204 scores serve as dynamic weights that scale the original TCN outputs, effectively enhancing influential
205 hydrological signals while suppressing less relevant temporal features.

206 **2.3.3 Feature-wise linear modulation for contextualization**

207 Alongside the temporal dependencies captured by the TCN, the model incorporates a dense network to
208 process static catchment attributes, ensuring physiographic and geospatial characteristics inform
209 streamflow predictions. To effectively integrate static catchment attributes into the temporal modeling of



streamflow, the model employs FiLM. FiLM allows the network to adapt its learned representations of hydrological dynamics in response to catchment-specific properties (Perez et al., 2018). FiLM applies two modulation parameters to the TCN's output feature representations: a scaling factor and a shifting factor. The scaling factor adjusts the strength of the extracted temporal features, while the shifting factor modifies the baseline streamflow response, ensuring that the model accounts for regional hydrological differences. FiLM learns these modulation parameters through a multi-layer perceptron that maps static catchment descriptors to the learned transformation space. The scaling and shifting transformations allow the model to condition its temporal feature extraction on catchment attributes, ensuring that the learned representations capture regional differences in hydrological behavior.

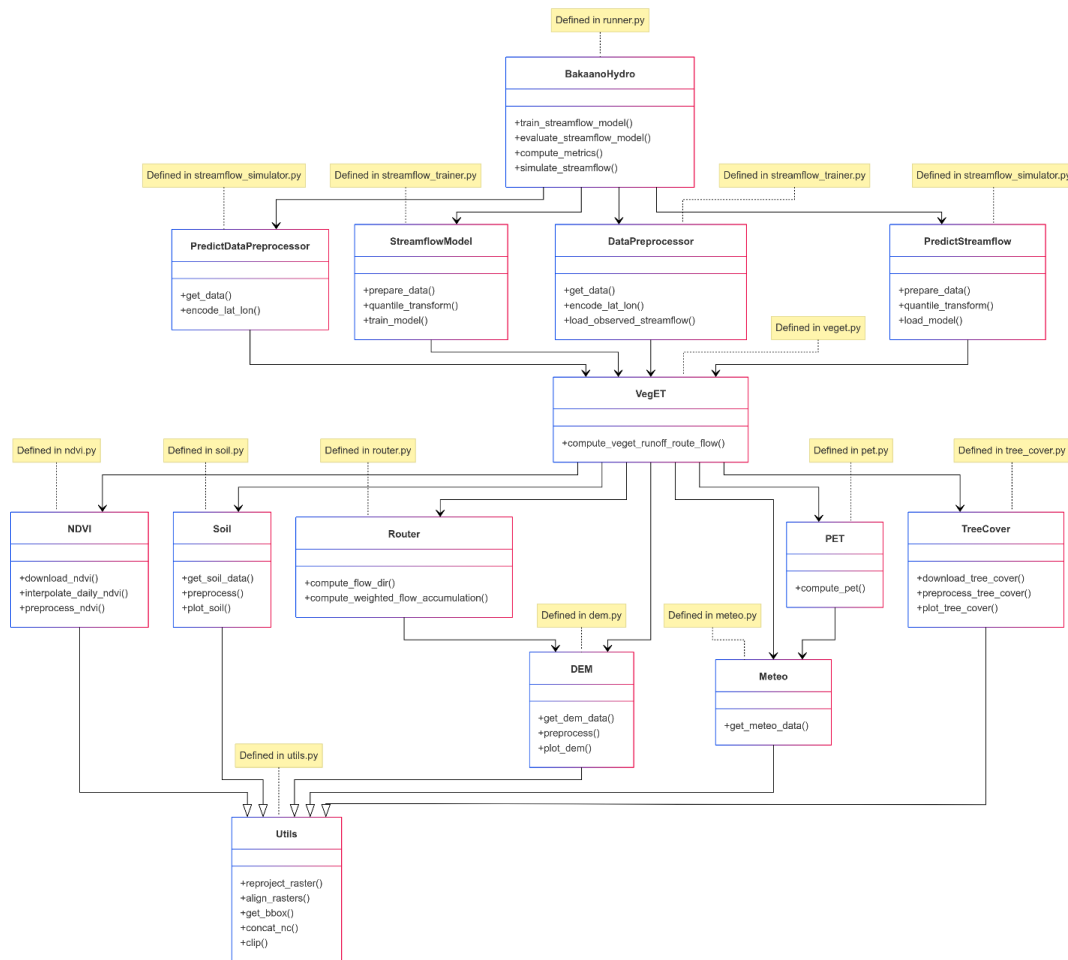
3. Bakaano-Hydro code architecture and workflow

Bakaano-Hydro follows an object-oriented architecture designed for modularity, scalability, and flexibility. The implementation is structured across multiple Python modules, each responsible for specific tasks within the hydrological simulation pipeline (Fig.3). The main module (*runner.py*) serves as the central workforce, managing gridded runoff simulation, topographic flow routing, sequential neural network training, and streamflow simulation. Data acquisition and preprocessing are executed separately from the main hydrological modeling components to ensure data reusability. Modules responsible for data retrieval and preprocessing include *meteo.py*, *tree_cover.py*, *dem.py*, *soil.py*, *ndvi.py*, and *utils.py*. These modules handle the downloading and processing of environmental variables such as meteorological data, vegetation indices, topography, and soil properties. The *meteo.py* module handles automated retrieval and preprocessing of gridded daily precipitation, maximum, minimum and mean temperature. Bakaano-Hydro allows for automated retrieval of these meteorological variables from three sources; ERA5-land (Muñoz-Sabater et al., 2021), CHIRPS (Funk et al., 2015) and the CHELSA-W5E5 database (Karger et al., 2023; Karger, 2021) in addition to the option for users to provide their own meteorological data. CHIRPS provides only daily precipitation data, as a result, temperature data are downloaded from ERA5-land if this option is selected. Unlike ERA5-land and CHIRPS, data availability from CHELSA is limited to the period 1981–2016. The *ndvi.py* module handles automated retrieval and preprocessing of NDVI data from MODIS (Didan, 2021; Dimiceli et al., 2015). The NDVI data are provided at 16-day intervals.

Following the VegET procedure, a daily mean climatology of NDVI for a specified period is established with linear interpolation (Senay et al., 2023). Soil properties, including wilting point, field capacity, and saturation, are retrieved from International Soil Reference and Information Center's SoilGrid database



240 (Poggio et al., 2021) using the *soil.py* module. DEM is sourced from HydroSHEDS (Lehner et al., 2008),
241 providing hydrologically corrected topographic data. Users can also provide their own elevation data.
242 Fractional tree and herbaceous cover at annual time-step are retrieved from the MODIS (Dimiceli et al.,
243 2015) using the *tree_cover.py* module. Because Bakaano-Hydro operates at the spatial resolution of the
244 elevation data, all input data are regridded to match the DEM data. The separation of data handling from
245 model execution allows flexibility in using the processed datasets for multiple modeling scenarios without
246 redundant computations. Hydrological simulations are managed through distinct process-based
247 components.



248

249 **Figure 3.** Bakaano-Hydro code structure, showing the modular design and interdependencies across
250 components. Modules are grouped by functionality, with each class defined in a separate Python script.



251 The *veget.py* module implements the VegET method for runoff generation. Flow routing is handled by
252 *router.py*, ensuring the representation of hydrological connectivity across upstream and downstream
253 regions. Training and simulation are executed within *streamflow_trainer.py* for model optimization and
254 *streamflow_simulator.py* for hydrological predictions. The modular design of Bakaano-Hydro ensures that
255 different components can be updated or replaced independently, promoting extensibility and
256 interoperability with various modeling approaches.

257 Deploying Bakaano-Hydro requires three primary data or inputs from a user. First, a shapefile of the river
258 basin or study area. Second, registration at Google Earth Engine
259 (<https://code.earthengine.google.com/register>). Bakaano-Hydro retrieves, NDVI, tree cover, herbaceous
260 cover and meteorological variables from ERA5-land or CHIRPS from Google Earth Engine Data Catalog. This
261 platform requires prior registration for subsequent authentication during execution of the model. Finally,
262 observed streamflow data in NetCDF format from Global Runoff Data Center (GRDC) (GRDC, 2025) .
263 Because Bakaano-Hydro aims to use only open-source data, it currently accepts observed streamflow data
264 only from GRDC. Subsequently, training and using the model for simulations consists of five steps. First,
265 data retrieval and preprocessing. This involves regridding and reprojection where necessary. Second, runoff
266 generation with VegET and subsequent routing through a river network. Third, training a model instance
267 based on specified training period. Fourth, evaluating the trained model on out-of-sample data. Finally,
268 applying the trained and evaluated model for subsequent simulation, scenario analysis etc.

269 **4. Application examples and diagnostic evaluation**

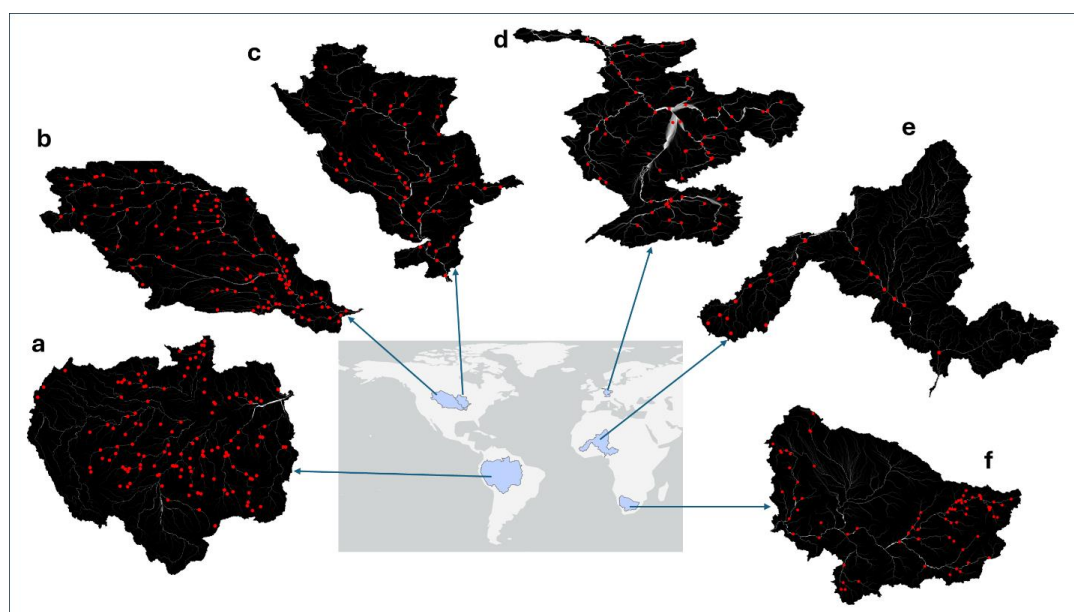
270 To evaluate the robustness and generalizability of the model, Bakaano-Hydro was deployed across six river
271 basins of varying sizes spanning four continents and representing a broad range of hydroclimatic, ecological
272 and land use conditions. They include the Amazon, Niger, Orange, Missouri, Upper Mississippi, and Rhine
273 basins (Fig. 4). These basins encompass highly contrasting environmental regimes, providing a rigorous
274 testbed for model performance.

275 **4.1. Study areas**

276 Figure 4 shows the location of the river basins and the hydrological stations used in training and evaluating
277 the model in each basin. The Amazon basin, with an area of approximately 7,000,000 km², is characterized
278 by humid tropical rainforest with year-round precipitation and high runoff. It represents a perennial,
279 energy-limited hydrological regime with minimal human regulation. The Niger river basin, with an area of



280 about 2,000,000 km², is a semi-arid to sub-humid system with strong rainfall seasonality, delayed runoff,
281 and substantial variability in flow timing and volume. It is particularly relevant for assessing model
282 performance under seasonal water scarcity and lagged hydrological responses. The Orange river basin,
283 with an area of approximately 973,000km², is a predominantly semi-arid system with low and highly
284 variable rainfall, frequent dry spells, and episodic high-intensity rainfall events that generate sharp
285 streamflow peaks. The basin is heavily regulated, and its runoff dynamics are influenced by both climatic
286 extremes and water management infrastructure, making it a useful test case for model performance under
287 arid and drought-prone conditions. Missouri river basin, with an area of about 1,400,000 km², is a snow-
288 dominated basin originating in the Rocky Mountains and flowing through semi-arid to temperate plains.



289

290 **Figure 4.** Maps showing the location of the river basins and the hydrological stations used in training and
291 evaluating model performance: **a)** is Amazon river basin; **b)** is Missouri basin; **c)** is Upper Mississippi basin;
292 **d)** is Rhine basin; **e)** is Niger basin and **f)** is Orange basin.

293

294 Upper Mississippi Basin, with an area of about 500,000 km², is a mixed snow and rain-fed basin with
295 temperate climate, extensive agricultural land use, and moderate hydrological regulation. It offers a
296 contrasting test case for evaluating model performance in intensively managed, mid-latitude catchments.
297 Rhine Basin, with an area of approximately 185,000km², is a temperate, well-instrumented basin with both
298 rain and snowmelt contributions, heavily influenced by urbanization and water management



299 infrastructure. It represents a densely monitored system with well-known anthropogenic impacts.
300 Together, these basins cover a spectrum of climate zones (humid tropical to semi-arid and temperate), flow
301 regimes (perennial, seasonal, snowmelt-dominated, and regulated), and land cover types (forest, savanna,
302 cropland, and urbanized areas).

303 **4.2. Model configuration**

304 For each basin, the relevant Bakaano-Hydro modules were used to automatically download and preprocess
305 input data. Meteorological data was obtained from the CHELSA-W5E5 database for all basins. The analysis
306 period was set from 1981 to 2016, aligning with the availability of the CHELSA-W5E5 data, which extends
307 until 2016. Observed streamflow data were obtained from the GRDC (GRDC, 2025). The spatial resolution
308 for all analysis was 1km². Hydrological stations were included in the analysis only if they had at least three
309 years of observed records within the study period and a catchment area greater than 1000 km². Based on
310 this criteria, 19 stations were selected for the Niger, 64 for the Upper Mississippi, 68 for the Rhine, and 131
311 for the Amazon, 53 for the Orange basin and 115 stations for the Missouri basin. Observed streamflow
312 records for each station were split into training (1989–2016) and independent evaluation (1982–1988)
313 periods. Due to variations in record lengths among stations, the number of stations available for training
314 and evaluation differed from the total number initially selected. The three-input branch architecture was
315 used for the Niger basin because it provided the best performance. For the rest of the basins, the two-
316 input branch configuration provided the best performance.

317 **4.3 Performance and diagnostic evaluation**

318 Model performance across hydroclimatic gradients was evaluated using a suite of diagnostic metrics that
319 characterize different aspects of streamflow simulation. The raincloud plots (Fig.5) reveal distinct patterns
320 of model behavior across the six selected basins, reflecting how climatic and hydrological conditions
321 influence predictive skill. Overall performance was assessed using the Nash–Sutcliffe Efficiency (NSE) and
322 the Kling–Gupta Efficiency (KGE). These metrics evaluate the ability of the model to capture the magnitude
323 and timing of streamflow. In humid and temperate basins such as the Amazon, Rhine, and Upper
324 Mississippi, both NSE and KGE values were high and tightly distributed across stations, indicating strong
325 and stable model performance (Fig.5). The Niger basin, though semi-arid to sub-humid, also showed
326 consistently positive NSE and KGE values with limited spread, suggesting robust performance under
327 seasonally dry conditions. In contrast, broader variability and lower median values were observed in the



Missouri and Orange basins, where snowmelt processes, episodic rainfall, and regulation introduce greater hydrological complexity and less predictable flow regimes.

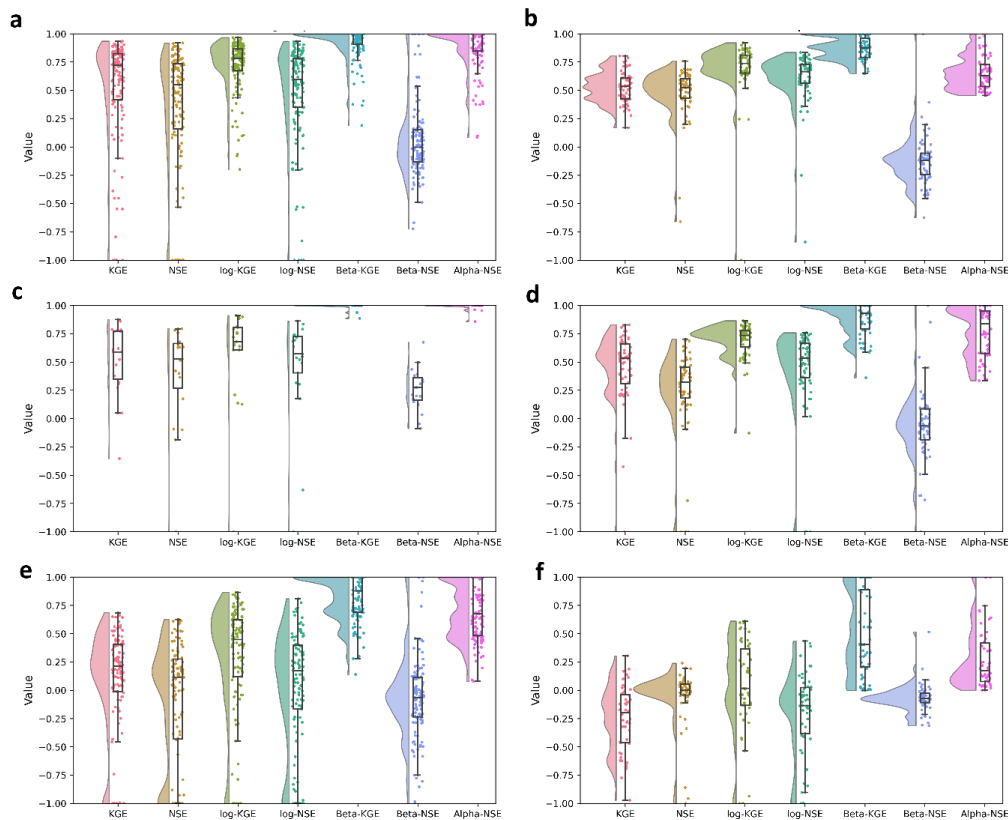
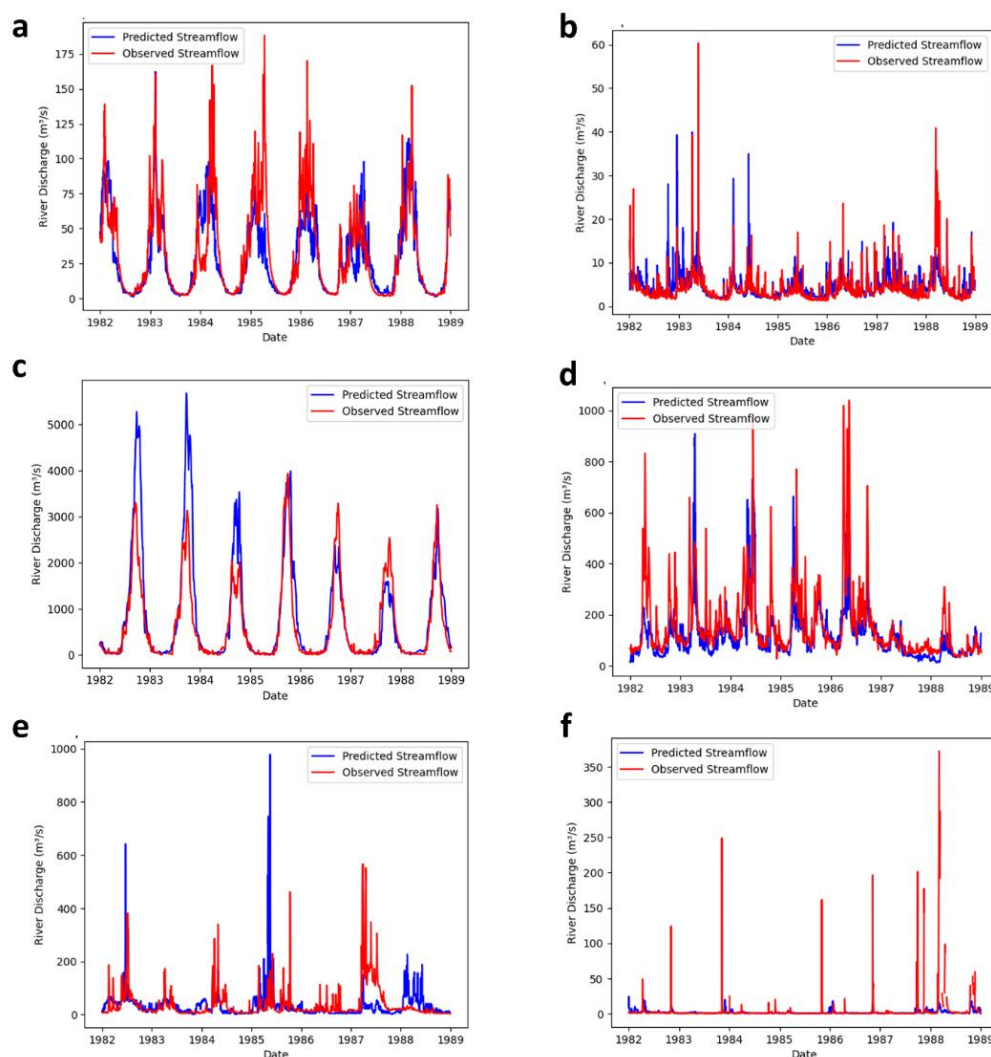


Figure 5. Performance evaluation of Bakaano-Hydro across multiple river basins; a is Amazon river basin, b is Rhine basin, c is Niger basin, d is Upper Mississippi basin, e is Missouri basin and f is Orange basin. The evaluation shows performance across multiple metrics KGE is NSE is . Each panel presents half violin plot, boxplots and density plots to visualize the distribution of the seven metrics. The boxplot shows distribution quartiles and whiskers show the full range; the points show the distribution for the gauging stations and the half-violin plots show the distribution density. The evaluation period was from 1982 to 1989 for each station and was not included during training for each basin.

To assess Bakaano-Hydro performance under low-flow conditions, log-transformed versions of NSE and KGE were used. Once again, the Amazon, Rhine, and Upper Mississippi basins showed strong results, with high log-KGE and log-NSE values and narrow distributions. Niger also performed adequately in low-flow periods, though with more variation in log-NSE, indicating occasional underestimation of recession flows.



343

344 **Figure 6.** Hydrographs of stations with the median KGE during the evaluation in each river basin: a) is
 345 Amazon river basin; b) is Rhine basin; c) is Niger basin; d) is Upper Mississippi basin; e) is Missouri basin
 346 and f) is Orange basin. The evaluation period was from 1982 to 1989 for each station and was not included
 347 during training for each basin.

348

349 Performance in the Orange and Missouri basins was notably weaker, consistent with the challenge of
 350 capturing low, variable flows in dryland or snow-affected systems (Fig.6). Model bias was analyzed using
 351 the Beta-KGE and Beta-NSE components. Beta-KGE values were consistently close to 1 across all basins,



352 indicating that the model accurately reproduces mean discharge with low absolute bias. However, Beta-
353 NSE values were generally lower and more variable, particularly in the Missouri and Orange basins. This
354 discrepancy reflects the fact that while the absolute bias may be small, it is large relative to the natural
355 variability of observed flows in these regions. The Alpha-NSE metric was used to assess how well the model
356 captures streamflow variability. Alpha values close to 1 indicate a good match between the standard
357 deviation of observed and simulated flows. Performance was strongest in the Amazon, Rhine, and Upper
358 Mississippi, where Alpha-NSE values were high and consistent across stations. The Niger basin also showed
359 strong performance, reflecting the model's ability to reproduce seasonal variability. Lower and more
360 variable Alpha-NSE values in the Missouri and Orange basins suggest that the model tends to
361 underestimate variability in streamflow. VegET uses a saturation-excess runoff generation mechanism,
362 where runoff occurs only after soil saturation. The simulated runoff is subsequently routed and fed into the
363 neural network component to predict streamflow. This configuration is particularly effective in humid,
364 energy-limited basins with frequent rainfall and sustained soil moisture, where saturation-excess dynamics
365 align with observed runoff generation processes (Beven, 2012; Kidron, 2021; Dunne and Black, 1970; Chow
366 et al., 1988). However, in semi-arid or subtropical basins such as the Orange and parts of the Missouri,
367 where rainfall is infrequent and intense, and soils are often dry or hydrophobic, runoff is more likely
368 generated through infiltration-excess (Hortonian) mechanisms (Chow et al., 1988; Kidron, 2021; Beven,
369 2012). Because VegET does not initiate runoff until the soil is saturated, it may fail to simulate rapid runoff
370 events triggered by high-intensity storms, leading to underestimation of peaks and timing errors. During
371 extended dry periods, soil moisture remains well below saturation thresholds, resulting in negligible runoff
372 even when surface runoff may occur in reality. These limitations hinder the neural network's ability to
373 reproduce sharp hydrograph responses in water-limited systems.

374 Overall, the diagnostic evaluation highlights a key structural constraint: the model performs best in humid
375 or temperate basins where saturation-excess runoff processes dominate and flow regimes are gradual and
376 persistent. In contrast, performance declines in dry or snow-affected basins with intermittent or threshold-
377 driven hydrology. Despite these limitations, the model demonstrates strong potential for cross-regional
378 application, particularly in environments where vegetation, soil moisture, and water availability interact
379 predictably to drive runoff production as well as in data-scarce basins (Fig.7). This supports its broader
380 utility in global-scale hydrological modeling, especially when complemented by improvements that
381 incorporate infiltration-excess processes or hybrid runoff generation schemes.

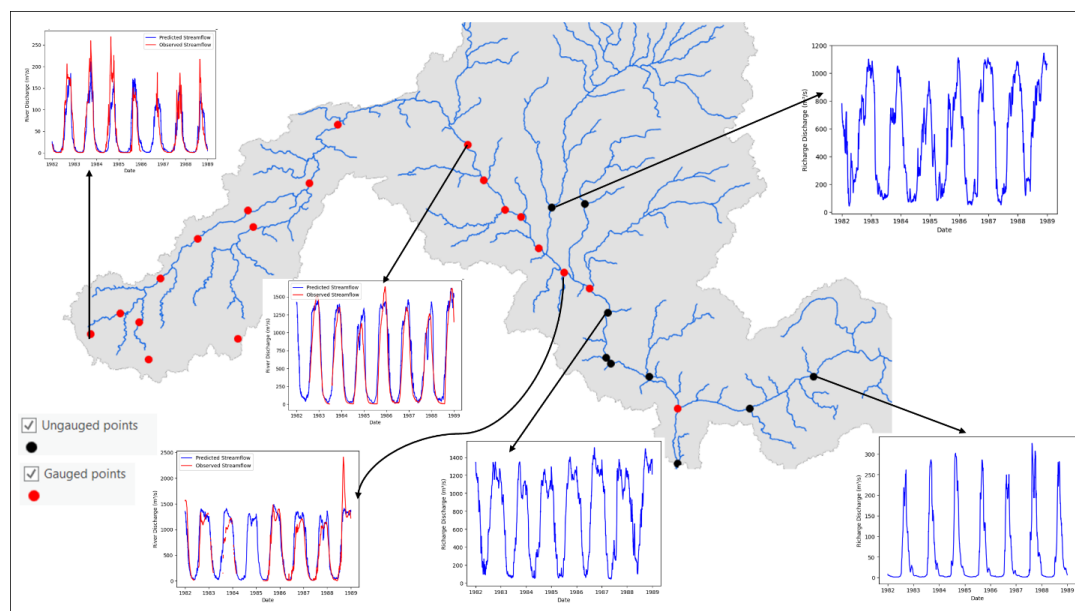


Figure 7. Demonstration of Bakaano-Hydro’s fully distributed streamflow prediction capability across a river basin. The map shows gauged points (red circles) used for training and evaluation and ungauged prediction points (black circles). Insets illustrate predicted vs. observed streamflow hydrographs at selected gauged during the evaluation period and predicted streamflow hydrographs at ungauged locations, highlighting the model’s ability to generalize across space and provide reliable streamflow estimates at any point within the basin.

5. Conclusions

This paper presents Bakaano-Hydro, a fully distributed hybrid modeling framework that integrates physically based runoff generation, topographic flow routing, and deep learning-based streamflow prediction. By coupling gridded process-based components with a temporal neural network architecture, the model effectively captures spatial heterogeneity, hydrological connectivity, and temporal dynamics within a cohesive structure. In contrast to traditional lumped or semi-distributed data-driven approaches, Bakaano-Hydro enables spatially explicit streamflow prediction at any location within a basin, informed by physically meaningful processes. The model was evaluated across six river basins of varying sizes, spanning four continents and representing diverse hydroclimatic regimes and land-use patterns. Results demonstrate strong predictive skill in humid, snow-fed, and seasonally dynamic systems, and consistent



401 generalization across basins of varying size and complexity. Performance was highest in catchments
402 dominated by saturation-excess runoff, while reduced accuracy in dryland basins highlights the need for
403 future integration of infiltration-excess processes to enhance robustness in arid environments. By
404 embedding hydrological realism within a data-driven framework, Bakaano-Hydro enhances interpretability
405 and improves generalizability—key advantages for next-generation streamflow modeling. Importantly,
406 Bakaano-Hydro is modular, fully automated, and open-source, allowing users to easily deploy it in new
407 regions or for new scenarios. These features make the framework particularly well-suited for application
408 in data-scarce regions, where conventional physically based models may be hindered by parameter
409 uncertainty and limited calibration data. With minimal tuning, the model can be used to generate reliable
410 streamflow predictions in poorly monitored catchments, offering a valuable tool for regions where water-
411 related decision-making is often most urgent but least supported by data infrastructure. Beyond its use in
412 research, Bakaano-Hydro offers strong potential for operational and policy-relevant applications, including
413 real-time streamflow forecasting, climate impact assessments, drought and flood risk monitoring, and
414 long-term adaptation planning. In future work, we aim to extend Bakaano-Hydro by incorporating
415 infiltration-excess, integrating uncertainty quantification, and enhancing coupling with land surface or
416 vegetation models. Together, these additions will further improve the model's robustness, transparency,
417 and applicability to a wider range of hydrological settings and societal needs. The source code is publicly
418 available at <https://github.com/confidence-duku/bakaano-hydro> to support reproducibility, collaborative
419 development, and wider adoption by the hydrological modeling and Earth system science communities.

420 **Code availability**

421 The minted version of Bakaano-Hydro v1.1 is available on Zenodo at
422 <https://doi.org/10.5281/zenodo.15227201>. Bakaano-Hydro is also available on GitHub at
423 <https://github.com/confidence-duku/bakaano-hydro>. The *README.md* file on
424 <https://github.com/confidence-duku/bakaano-hydro> provides documentation on installation and usage
425 requirements. The *requirements.txt* also on GitHub <https://github.com/confidence-duku/bakaano-hydro>
426 provides details on the required dependencies. Additionally, a Jupyter Notebook, *quick_start.ipynb*, is
427 available and provides a stepwise guidance to the full Bakaano-Hydro pipeline from download to model
428 training and simulation.

429 **Data availability**

430 Meteorological data for the six case studies are available from



431 <https://doi.org/10.48364/ISIMIP.836809.2> (Karger, 2021). Tree cover and herbaceous cover data are
432 available from
433 https://developers.google.com/earth-engine/datasets/catalog/MODIS_061_MOD44B#bands (Dimiceli et
434 al., 2015). NDVI data are available from
435 https://developers.google.com/earth-engine/datasets/catalog/MODIS_061_MOD13A2 (Didan, 2015).
436 Soil data are available from <https://files.isric.org/soilgrids/> (Poggio et al., 2021). Elevation data are
437 available from https://data.hydrosheds.org/file/hydrosheds-v1-dem/hyd_glo_dem_30s.zip (Lehner et al.,
438 2008). Observed streamflow data are available from
439 <https://portal.grdc.bafg.de/applications/public.html?publicuser=PublicUser#dataDownload/Home> (Grdc,
440 2025).

441 Competing interests

442 The author declares no conflict of interest.

443 Reference

- 444 Anderson, S. and Radić, V.: Evaluation and interpretation of convolutional long short-term memory
445 networks for regional hydrological modelling, *Hydrol. Earth Syst. Sci.*, 26, 795-825, 10.5194/hess-
446 26-795-2022, 2022.
- 447 Arnold, J. G., Srinivasan, R., Muttiah, R. S., and Williams, J. R.: Large area hydrologic modeling and
448 assessment part I: model development 1, *JAWRA Journal of the American Water Resources*
449 *Association*, 34, 73-89, 1998.
- 450 Arsenault, R., Martel, J. L., Brunet, F., Brissette, F., and Mai, J.: Continuous streamflow prediction in
451 ungauged basins: long short-term memory neural networks clearly outperform traditional
452 hydrological models, *Hydrol. Earth Syst. Sci.*, 27, 139-157, 10.5194/hess-27-139-2023, 2023.
- 453 Bai, S., Kolter, J. Z., and Koltun, V.: An empirical evaluation of generic convolutional and recurrent
454 networks for sequence modeling. *arXiv, arXiv preprint arXiv:1803.01271*, 10, 2018.
- 455 Beven, K. J.: *Rainfall-runoff modelling: the primer*, John Wiley & Sons 2012.
- 456 Cassagnole, M., Ramos, M. H., Zalachori, I., Thirel, G., Garçon, R., Gailhard, J., and Ouillon, T.: Impact of
457 the quality of hydrological forecasts on the management and revenue of hydroelectric reservoirs
458 – a conceptual approach, *Hydrol. Earth Syst. Sci.*, 25, 1033-1052, 10.5194/hess-25-1033-2021,
459 2021.
- 460 Chow, V. T., Maidment, D. R., and Mays, L. W.: *Applied Hydrology*, MacGraw-Hill, Inc., New York, 572,
461 1988.
- 462 De Roo, A. P. J., Wesseling, C. G., and Van Deursen, W. P. A.: Physically based river basin modelling within
463 a GIS: the LISFLOOD model, *Hydrological Processes*, 14, 1981-1992,
464 [https://doi.org/10.1002/1099-1085\(20000815/30\)14:11/12<1981::AID-HYP49>3.0.CO;2-F](https://doi.org/10.1002/1099-1085(20000815/30)14:11/12<1981::AID-HYP49>3.0.CO;2-F), 2000.
- 465 Depetris, P. J.: The Importance of Monitoring River Water Discharge, *Frontiers in Water*, 3,
466 10.3389/frwa.2021.745912, 2021.
- 467 Didan, K.: MOD13A2 MODIS/terra vegetation indices 16-day L3 global 1km SIN grid V006, (No Title),
468 2015.



- 469 Didan, K.: MODIS/Terra Vegetation Indices 16-Day L3 Global 250m SIN Grid V061 [Data set]. NASA EOSDIS
470 Land Processes Distributed Active Archive Center, Accessed 2023-11-09 from [https://doi.](https://doi.org/10.5067/MODIS/MOD13Q1.061)
471 [org/10.5067/MODIS/MOD13Q1.061](https://doi.org/10.5067/MODIS/MOD13Q1.061), 2021.
- 472 DiMiceli, C., Carroll, M., Sohlberg, R., Kim, D.-H., Kelly, M., and Townshend, J.: MOD44B MODIS/Terra
473 vegetation continuous fields yearly L3 global 250m SIN grid V006, NASA EOSDIS Land Processes
474 DAAC, 10, 2015.
- 475 Dunne, T. and Black, R. D.: Partial area contributions to storm runoff in a small New England watershed,
476 Water resources research, 6, 1296-1311, 1970.
- 477 Funk, C., Peterson, P., Landsfeld, M., Pedreros, D., Verdin, J., Shukla, S., Husak, G., Rowland, J., Harrison,
478 L., Hoell, A., and Michaelsen, J.: The climate hazards infrared precipitation with stations—a new
479 environmental record for monitoring extremes, Scientific Data, 2, 150066,
480 10.1038/sdata.2015.66, 2015.
- 481 Gauch, M., Kratzert, F., Klotz, D., Nearing, G., Lin, J., and Hochreiter, S.: Rainfall–runoff prediction at
482 multiple timescales with a single Long Short-Term Memory network, Hydrol. Earth Syst. Sci., 25,
483 2045-2062, 10.5194/hess-25-2045-2021, 2021.
- 484 Golden, H. E., Christensen, J. R., McMillan, H. K., Kelleher, C. A., Lane, C. R., Husic, A., Li, L., Ward, A. S.,
485 Hammond, J., Seybold, E. C., Jaeger, K. L., Zimmer, M., Sando, R., Jones, C. N., Segura, C.,
486 Mahoney, D. T., Price, A. N., and Cheng, F.: Advancing the science of headwater streamflow for
487 global water protection, Nature Water, 3, 16-26, 10.1038/s44221-024-00351-1, 2025.
- 488 GRDC: The Global Runoff Data Centre, 56068 Koblenz, Germany (<https://grdc.bafg.de/>), 2025.
- 489 Hamman, J. J., Nijssen, B., Bohn, T. J., Gergel, D. R., and Mao, Y.: The Variable Infiltration Capacity model
490 version 5 (VIC-5): infrastructure improvements for new applications and reproducibility, Geosci.
491 Model Dev., 11, 3481-3496, 10.5194/gmd-11-3481-2018, 2018.
- 492 Hargreaves, G. H. and Samani, Z. A.: Reference crop evapotranspiration from temperature, Applied
493 engineering in agriculture, 1, 96-99, 1985.
- 494 Herrera, D., Ellis, A., Fisher, B., Golden, C. D., Johnson, K., Mulligan, M., Pfaff, A., Treuer, T., and Ricketts, T.
495 H.: Upstream watershed condition predicts rural children’s health across 35 developing countries,
496 Nature Communications, 8, 811, 10.1038/s41467-017-00775-2, 2017.
- 497 Herrera, P. A., Marazuela, M. A., and Hofmann, T.: Parameter estimation and uncertainty analysis in
498 hydrological modeling, WIREs Water, 9, e1569, <https://doi.org/10.1002/wat2.1569>, 2022.
- 499 Hunt, K. M. R., Matthews, G. R., Pappenberger, F., and Prudhomme, C.: Using a long short-term
500 memory (LSTM) neural network to boost river streamflow forecasts over the western United
501 States, Hydrol. Earth Syst. Sci., 26, 5449-5472, 10.5194/hess-26-5449-2022, 2022.
- 502 Ioffe, S. and Szegedy, C.: Batch normalization: Accelerating deep network training by reducing internal
503 covariate shift, International conference on machine learning, 448-456,
- 504 Karger, D. N., Lange, S., Hari, C., Reyer, C. P. O., Conrad, O., Zimmermann, N. E., and Frieler, K.: CHELSA-
505 W5E5: daily 1 km meteorological forcing data for climate impact studies, Earth Syst. Sci. Data, 15,
506 2445-2464, 10.5194/essd-15-2445-2023, 2023.
- 507 Karger, D. N. L., S; Hari, C.; Reyer, P. O. C.; Zimmermann, E. N.: CHELSA-W5E5 v1.1: W5E5 v1.0
508 downscaled with CHELSA v2.0, ISIMIP Repository. [dataset], 2021.
- 509 Kidron, G. J.: Comparing overland flow processes between semiarid and humid regions: Does saturation
510 overland flow take place in semiarid regions?, Journal of Hydrology, 593, 125624,
511 <https://doi.org/10.1016/j.jhydrol.2020.125624>, 2021.
- 512 Kratzert, F., Klotz, D., Brenner, C., Schulz, K., and Herrnegger, M.: Rainfall–runoff modelling using Long
513 Short-Term Memory (LSTM) networks, Hydrol. Earth Syst. Sci., 22, 6005-6022, 10.5194/hess-22-
514 6005-2018, 2018.



- 515 Kratzert, F., Klotz, D., Shalev, G., Klambauer, G., Hochreiter, S., and Nearing, G.: Towards learning
516 universal, regional, and local hydrological behaviors via machine learning applied to large-sample
517 datasets, *Hydrol. Earth Syst. Sci.*, 23, 5089-5110, 10.5194/hess-23-5089-2019, 2019.
- 518 Lehner, B., Verdin, K., and Jarvis, A.: New Global Hydrography Derived From Spaceborne Elevation Data,
519 *Eos, Transactions American Geophysical Union*, 89, 93-94,
520 <https://doi.org/10.1029/2008EO100001>, 2008.
- 521 Luong, M.-T., Pham, H., and Manning, C. D.: Effective approaches to attention-based neural machine
522 translation, *arXiv preprint arXiv:1508.04025*, 2015.
- 523 Moges, E., Demissie, Y., Larsen, L., and Yassin, F.: Review: Sources of Hydrological Model Uncertainties
524 and Advances in Their Analysis, *Water*, 13, 28, 2021.
- 525 Muñoz-Sabater, J., Dutra, E., Agustí-Panareda, A., Albergel, C., Arduini, G., Balsamo, G., Boussetta, S.,
526 Choulga, M., Harrigan, S., Hersbach, H., Martens, B., Miralles, D. G., Piles, M., Rodríguez-
527 Fernández, N. J., Zsoter, E., Buontempo, C., and Thépaut, J. N.: ERA5-Land: a state-of-the-art
528 global reanalysis dataset for land applications, *Earth Syst. Sci. Data*, 13, 4349-4383, 10.5194/essd-
529 13-4349-2021, 2021.
- 530 Nearing, G., Cohen, D., Dube, V., Gauch, M., Gilon, O., Harrigan, S., Hassidim, A., Klotz, D., Kratzert, F.,
531 Metzger, A., Nevo, S., Pappenberger, F., Prudhomme, C., Shalev, G., Shenzi, S., Tekalign, T. Y.,
532 Weitzner, D., and Matias, Y.: Global prediction of extreme floods in ungauged watersheds,
533 *Nature*, 627, 559-563, 10.1038/s41586-024-07145-1, 2024.
- 534 Palmer, M. and Ruhi, A.: Linkages between flow regime, biota, and ecosystem processes: Implications for
535 river restoration, *Science*, 365, eaaw2087, doi:10.1126/science.aaw2087, 2019.
- 536 Perez, E., Strub, F., De Vries, H., Dumoulin, V., and Courville, A.: Film: Visual reasoning with a general
537 conditioning layer, *Proceedings of the AAAI conference on artificial intelligence*,
- 538 Poggio, L., de Sousa, L. M., Batjes, N. H., Heuvelink, G. B. M., Kempen, B., Ribeiro, E., and Rossiter, D.:
539 SoilGrids 2.0: producing soil information for the globe with quantified spatial uncertainty, *SOIL*, 7,
540 217-240, 10.5194/soil-7-217-2021, 2021.
- 541 Quinn, P., Beven, K., Chevallier, P., and Planchon, O.: The prediction of hillslope flow paths for distributed
542 hydrological modelling using digital terrain models, *Hydrological processes*, 5, 59-79, 1991.
- 543 Schaphoff, S., von Bloh, W., Rammig, A., Thonicke, K., Biemans, H., Forkel, M., Gerten, D., Heinke, J.,
544 Jägermeyr, J., Knauer, J., Langerwisch, F., Lucht, W., Müller, C., Rolinski, S., and Waha, K.: LPJmL4 –
545 a dynamic global vegetation model with managed land – Part 1: Model description, *Geosci.*
546 *Model Dev.*, 11, 1343-1375, 10.5194/gmd-11-1343-2018, 2018.
- 547 Senay, G. B.: Modeling Landscape Evapotranspiration by Integrating Land Surface Phenology and a Water
548 Balance Algorithm, *Algorithms*, 1, 52-68, 2008.
- 549 Senay, G. B., Kagone, S., Parrish, G. E. L., Khand, K., Boiko, O., and Velpuri, N. M.: Improvements and
550 Evaluation of the Agro-Hydrologic VegET Model for Large-Area Water Budget Analysis and
551 Drought Monitoring, *Hydrology*, 10, 168, 2023.
- 552 Shi, X., Chen, Z., Wang, H., Yeung, D.-Y., Wong, W.-K., and Woo, W.-c.: Convolutional LSTM network: A
553 machine learning approach for precipitation nowcasting, *Advances in neural information*
554 *processing systems*, 28, 2015.
- 555 Srivastava, N., Hinton, G., Krizhevsky, A., Sutskever, I., and Salakhutdinov, R.: Dropout: a simple way to
556 prevent neural networks from overfitting, *The journal of machine learning research*, 15, 1929-
557 1958, 2014.
- 558 Yu, Q., Tolson, B. A., Shen, H., Han, M., Mai, J., and Lin, J.: Enhancing long short-term memory (LSTM)-
559 based streamflow prediction with a spatially distributed approach, *Hydrol. Earth Syst. Sci.*, 28,
560 2107-2122, 10.5194/hess-28-2107-2024, 2024.

561